

Comparative Study of Microinverters Topologies and Control Schemes for Photovoltaic Applications

(Kajian Perbandingan Topologi Mikroinverter dan Skim Kawalan untuk Aplikasi Fotovoltaik)

*MOHD FUAD OMAR¹, NOOR LAILA ASHA'ARI², AZLINDA SUBOH³

¹Jabatan Matematik, Sains & Komputer, Politeknik Tuanku Syed Sirajuddin, Pauh Putra, 02600, Arau, Perlis, Malaysia.

²Jabatan Kejuruteraan Elektrik, Politeknik Tuanku Syed Sirajuddin, Pauh Putra, 02600, Arau, Perlis, Malaysia.

³Jabatan Kejuruteraan Elektrik, Politeknik Kota Kinabalu, No. 4 Jalan Politeknik KKIP Barat, KKIP, 88460 Kota Kinabalu, Sabah, Malaysia.

* Corresponding author: mohdfuad@ptss.edu.my

ARTICLE INFO

Article History:

Received 19.06.2023

Accepted 14.07.2023

Published 23.11.2023

Abstract

Photovoltaic (PV) energy is one of the most promising emerging technologies for renewable energy sources. An alternative solution for photovoltaic (PV) generation systems is the grid-connected AC module. It combines the PV panel with the microinverter connected to the grid. A transformer is a key component of a grid-connected photovoltaic (PV) microinverters system regarding safety and power quality issues. The microinverter shall ensure that the maximum power operation of the PV module is carried out with the Maximum Power Point Tracking (MPPT) and Total Harmonic Distortion (THD) should not be more than 5% according to the standards of IEEE 1547 and IEC 6172. With the aid of the MATLAB Simulink software, the comparative study of double stage isolated microinverter topologies for PV systems is presented in this paper. The multistage microinverter consists of six isolated topologies of DC-DC converter with maximum power point tracking (MPPT) and H-bridge inverter. The control algorithms are implemented according to the Perturbation and Observation (P&O) method. The device switching is controlled by using MOSFET with a frequency value of 100kHz for converter switching and 20kHz for inverter switching. The designs made have met the requirements of $V_{out} = 230V$ (rms), $I_{out} = 0.923A$, $P_{out} = 300W$ and, output frequency = 50Hz. The design of microinverters modelled in this study is Fly-back, Interleaved Fly-back, Push-Pull, Current-Fed, Half Bridge, and Full-Bridge. As a result, by comparing all of the 6 topologies microinverters designed, the Flyback Microinverter was proposed. The THD rates for flyback microinverter is measured at 1.24% in FFT spectrum, and the transformer ratio value of 3.7 compared to other design.

Keywords: Microinverter, DC-DC Converter, H Bridge Inverter, Photovoltaic, Total Harmonic Distortion.

INTRODUCTION

One of the most widely used renewable energy sources nowadays is solar energy. There are several research conducted on photovoltaics (PVs) and solar energy systems. Using a solar photovoltaic (PV) cell, solar energy can be harvested as both thermal energy (heat) and electrical energy (Abd Rahim et al., 2016). The voltage and current output of a signal PV cell may be insufficient since the photovoltaic cell converts sunlight into electricity (Nanou & Papathanassiou, 2014). To achieve a voltage and current level adequate for practical usage, PV cells are linked in series or parallel. A more crucial tool for obtaining an AC power signal from renewable energy sources is the DC/AC inverter (Aboadla et al., 2016). The output voltage of renewable sources, such as solar cells or fuel cells, is increased to 380–400 V using the high step-up converter as a DC link to the electrical grid. To properly regulate the grid voltage level, a high step-up voltage gain DC-DC converter is needed because the single solar cell module and fuel cell stack are both fundamentally low voltage sources. (Chen et al., 2010). Compared to other renewable sources, solar energy has the benefit of being usable practically everywhere with the proper arrangement of PV arrays. (Latran & Teke, 2015). The micro inverter's purpose is to monitor how the system responds to changes in solar irradiation. PV Microinverters contain either a single or multi-stage power conditioning system, this primarily affects the control strategies in order to achieve grid appliance (Tali et al., 2014). Regarding power quality and safety concerns, galvanic insulation in grid-connected photovoltaic (PV) microinverters is a crucial component. (Hasan et al., 2017). However, the efficiency of isolated microinverter will reduce because of the high switching and high-frequency transformers losses. Several isolated topologies have recently been proposed to increase the efficiency and life of PV converters. To maximize the output energy of PV arrays, it is important to operate PV energy conversion systems in the maximum power point tracking (MPPT) (Nguyen et al., 2018). MPPT is a technique widely used to optimize power extraction under certain conditions in photovoltaic (PV) solar systems. MPPT is an algorithm used in the charge controllers used by the PV module to extract the maximum available power. The input voltage from the PV needs to step up from using a DC-DC converter (Tali et al., 2014). Isolated DC-DC converters will protect the source from high voltage variations at the load. Such converters offer effective utilization of the energy source, and wider load regulations and possess the capability to work with a broader variety of input voltages (Amir et al., 2019). The power decoupling capacitor or also known as the DC-Link capacitor is placed between the DC-DC converter and the inverter in the double-stage topology of microinverters. The main purposes of DC-link capacitors are to maintain a steady-state DC voltage with small ripples and serve as an aspect of energy storage to provide the real power difference during transients between load and source (Amir et al., 2019). In this application, DC-link capacitors absorb switching currents to achieve a minimum ripple voltage (Dwivedi et al., 2018). The capacitor must be sized to meet the DC-link ripple voltage requirements. The performance of these topologies is then compared with the predefined requirements and standards (Hasan et al., 2017). Most DC-AC converters or isolated DC-DC converters and many other kinds of power electronics devices use H bridges in PV applications. Power is shifted from a DC source from the DC link to an AC load in this analysis by using Unipolar PWM single-phase H-Bridge inverters (Adam, 2017). The Unipolar switching is chosen because the output voltage level varies from either 0 to -V or from 0 to +V in the Unipolar switching scheme (Aboadla et al., 2016). Compared to the bipolar-switching scheme, this scheme 'effectively' has the effect of doubling the switching frequency in terms of output harmonics. The MOSFET is used in DC-DC converters and inverters as a switch due to its faster switching speed (Dwivedi et al., 2018). It is usually used at frequencies ranging from several kHz to more than several hundred kHz as a switching device. MOSFET is chosen for the closed-form solution for better output current and voltage of PV cells and has been analyzed (Adam, 2017). Besides, the voltage through the MOSFET conducting would be much lower than that through a diode, resulting in lower losses (Amir et al., 2019). As their power consumption is very small, MOSFET's also suitable for use as electronic switches. The LC Low Pass Filter is used to reduce the harmonics found in the inverter output voltage and to create a clean

sinusoidal output voltage (Latran & Teke, 2015). It is placed between the inverter and the load in a PV system. The maximum ripple current in the inductor and ripple voltage of the capacitor which these components can tolerate are calculated by L & C. The values can depend on the inverter switching frequency and maximum currents. In this study, the PV system with a double stage microinverter topology is designed using the MATLAB Simulink software. The first step is made by designing the DC-DC converter, continuing with connecting the DC-DC converter with the inverter and filter. To boost and regulate the low output voltage of the PV, 6 types of DC-DC converters are reviewed and designed which are flyback, push-pull, interleaved flyback, half-bridge, full-bridge, and Current Fed DC-DC converter. The requirement of this initial experiment, the simulation was made using a 110 V DC supply source to produce 230V (rms), 300W and 50Hz at load. This initial experiment was to ensure that the design of the microinverter circuit works well and achieves a THD of less than 5%. The last step for this study is to replace the supply source with a PV module and MPPT. Comparison in terms of THD is made for all circuits to see the effects or changes that occur and then meet the requirements that have been set. A single-phase H-bridge inverter, on the other hand, carries out the dc-to-ac conversion operation, with an aiding modulation algorithm handling control. In this simulation, the attention will be concentrated on the perturbation and observation (P&O) classical method of MPPT. The solar intensity and cell temperature measurements as well as the perturbation and observation algorithm are straightforward, require no prior knowledge of the PV generator's properties, and are simple to implement using analog and digital circuitry. (Hart, 2011). The microinverter's dc-dc converter component is under the direction of the P&O MPPT algorithm, which quickly adapts to changes in irradiance.

METHODOLOGY

Fig. 1. shows the block diagram of a multi-stage isolated microinverter. This system consists of three modules of PV connected as series to produce the voltage, 110V and current, 5.17A. The circuits are composed of 6 types of DC-DC converters in the DC-DC stages and an H-bridge inverter in the DC-AC stage.

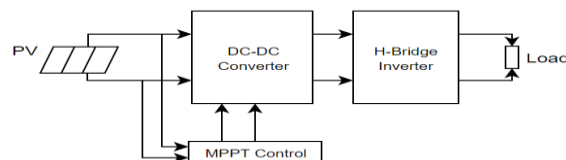


Fig. 1. Block Diagram of multistage isolated microinverter

DC-DC CONVERTER DESIGN

The DC-DC converter circuits were used in the microinverter to increase the voltage source from 110V up to 400V. All the DC-DC converter designs in microinverter were isolated types because they have some advantages compared to the transformer-less or non-isolated types of microinverter. In terms of cost, performance, and compactness, transformer-less or non-isolated converter types are superior (Hasan & Mekhilef, 2017). However, the existence of leakage ground current, the need for dual grounding, and the low voltage gain are the constraints on realizing them with PV modules (Hasan & Mekhilef, 2017). A capacitor is mounted on the output DC-DC converter or known as DC-link for the purpose of stabilizing the output voltage. In this study, six types of DC-DC converter circuits have been designed, namely Flyback converter, Interleaved Flyback converter, Push-Pull converter, Half-Bridge converter, Full-Bridge converter, and Current Fed converter.

The flyback converter is a kind of converter that provides isolation between input and output. This is because the circuit uses the transformer model which includes the

magnetizing inductance L_m . The basic operation of the flyback converter is similar to that of the buck-boost converter which energy is stored in L_m when the switch is closed and is then transferred to the load when the switch is open (Hart, 2011). Switch mode power supplies must work at high frequencies to use smaller and cheaper magnetic inductors and transformers to minimize energy and the expense of electronic devices (Nanou & Papathanassiou, 2014). Therefore, the value of the switching frequency selected is 100kHz. A flyback converter is depicted in Fig. 2 and is made up of a transformer, a switching MOSFET (Metal Oxide Semiconductor Field Effect Transistor), a freewheeling diode, and a PWM controller. To simplify the analysis of a flyback converter, the transformer model with magnetizing inductance L_m is included (Chen et al., 2014). The circuit operates in a steady state, which means that all voltages and currents over one switching cycle are periodic and start and stop at the same points. The duty ratio of the switch is D , being closed for time DT and open for $(1-D)T$. The last assumption is that the switch and diode are ideal. These are additional assumptions for the analysis. (Hart, 2011). The operation of a flyback converter can then be analyzed in both switching intervals.

The Interleaved Flyback dc-dc converter is made to minimize current ripple, meet galvanic isolation requirements, and reduce the turns ratio, switch voltage stress, and size of magnetic components. (Huber & Jovanovic, 1999). However, current sharing between parallel paths is a major design problem to be considered by using a parallel converter with interleaved power. Although highly consistent multichannel PWM signals can be produced by the commonly used control chips, the mismatch in the duty cycle is unavoidable due to the difference in the parameters of the drive circuits and the power switches (Huber & Jovanovic, 1999). Figure 2 b. shows the circuit Interleaved flyback dc-dc converter design. The design of this circuit consists of 2 flyback converters connected in parallel. These run at the same switching frequency, but the switches in the two converters are sequenced to switch apart from each other over a half-time cycle. In this study, the operating switching frequency is 100kHz by using MOSFET as a switch. The transformer ratio for these two converters is equal in value. The circuit operates via a voltage source of 110V to produce 400V.

Microinverters based on Push-pull converters have the advantages to reduce EM noise, relatively low semiconductor stress, and reduced passive component count (Wang et al., 2009). Fig. 2 c. shows a Push-pull converter circuit that consists of two MOSFETs as a switch (M1, M2) a center-tapped transformer, and four diodes (D1, D2, D3, D4). Both switches M1 and M2 are ground referenced that make simpler gate drive circuits and easy control of the power devices. While the switch M1 and M2 are alternately turned on and off, the power has been transferred to each primary of the center-tapped transformer. The transformer turns ratio has been designed to get a high voltage conversion ratio. Below is the equation of the output voltage of the push-pull converter.

$$(V_o) = 2V_s \left(\frac{N_2}{N_1} \right) D \quad (1)$$

The output ripple for the push-pull converter is:

$$\frac{\Delta V_o}{V_o} = \left(\frac{1-2D}{32L_x C(f)^2} \right) \quad (2)$$

The output of DC voltage then converts to AC using an H-bridge inverter.

The Current-fed converter is largely used by industry as battery chargers (Wang et al., 2009) or power factor correction circuits due to their good operational characteristics, such as no possibility of flux unbalance and good output cross-regulation. This converter is called a circuit that works by switching current rather than voltage (Adam, 2017). Fig. 2 d. shows a circuit of a current-fed converter that is a modification of the push-pull converter. The inductor L_m has been shifted from the transformer's output side to the input side. Switch 1 and Switch 2 close and open alternately to operate the diode. When switch

1 is closed and switch 2 is opened, the inductor current flows through the primary winding and through D1 and D4 on the secondary winding. D2 and D3 are currently off. When switch 2 is closed and switch 1 is opened, the inductor current flows through the primary winding and through D3 and D2 on the secondary winding. D1 and D4 currently are off. The output voltage, V_o can be expressed as below:

$$V_o = \frac{V_s}{2(1-D)} \left(\frac{N_s}{N_p} \right) \quad (3)$$

where D is the duty ratio of each switch.

A Half-bridge converter as shown in Fig. 2 e. is a type of DC-DC converter similar operation with Push-pull and Current-fed converters. Capacitors C1 and C2 are wide and equal value in the Half-bridge converter. Between the capacitors, the input voltage is distributed equally (Adam, 2017). The two switching components of the converter alternate back and forth, switching the voltage around the primary winding. A positive and negative voltage swing is thus encountered by the primary, which requires a full-wave bridge circuit for the output. The secondary side of the circuit operates at twice the frequency of the basic switching frequency because of its full-wave nature. While more complex than a flyback converter, the design of the half-bridge converter can generate higher output power and use smaller and less costly components.

A Full-bridge converter is one of the common topologies used attractively for high-power generation. A transformer is used in the isolated bridge converter to provide insulation in addition to stepping up the voltage. A Full-bridge converter is a DC-DC converter configuration that basically works with four active switching components around a power transformer in a bridge configuration (Pressman, 1991). In this study, a Full-bridge converter circuit consists of four MOSFETs as an active switching device. The operation of a Full-bridge converter involves switching one pair of MOSFET at one time for a half cycle of the control signal and the other pair switching during the other part of the signal at the value of high frequencies 20kHz. A full-bridge power converter (S1 to S4), a high-frequency transformer (with a ratio of 1:5), a bridge diode, and an output filter (L, C) are the components of the circuit schematic for a full-bridge converter shown in Fig. 2 f. A portion of each half cycle of switching frequency is used to alternately turn on and off the switches that are diagonally opposite (S1 and S4, or S2 and S3).

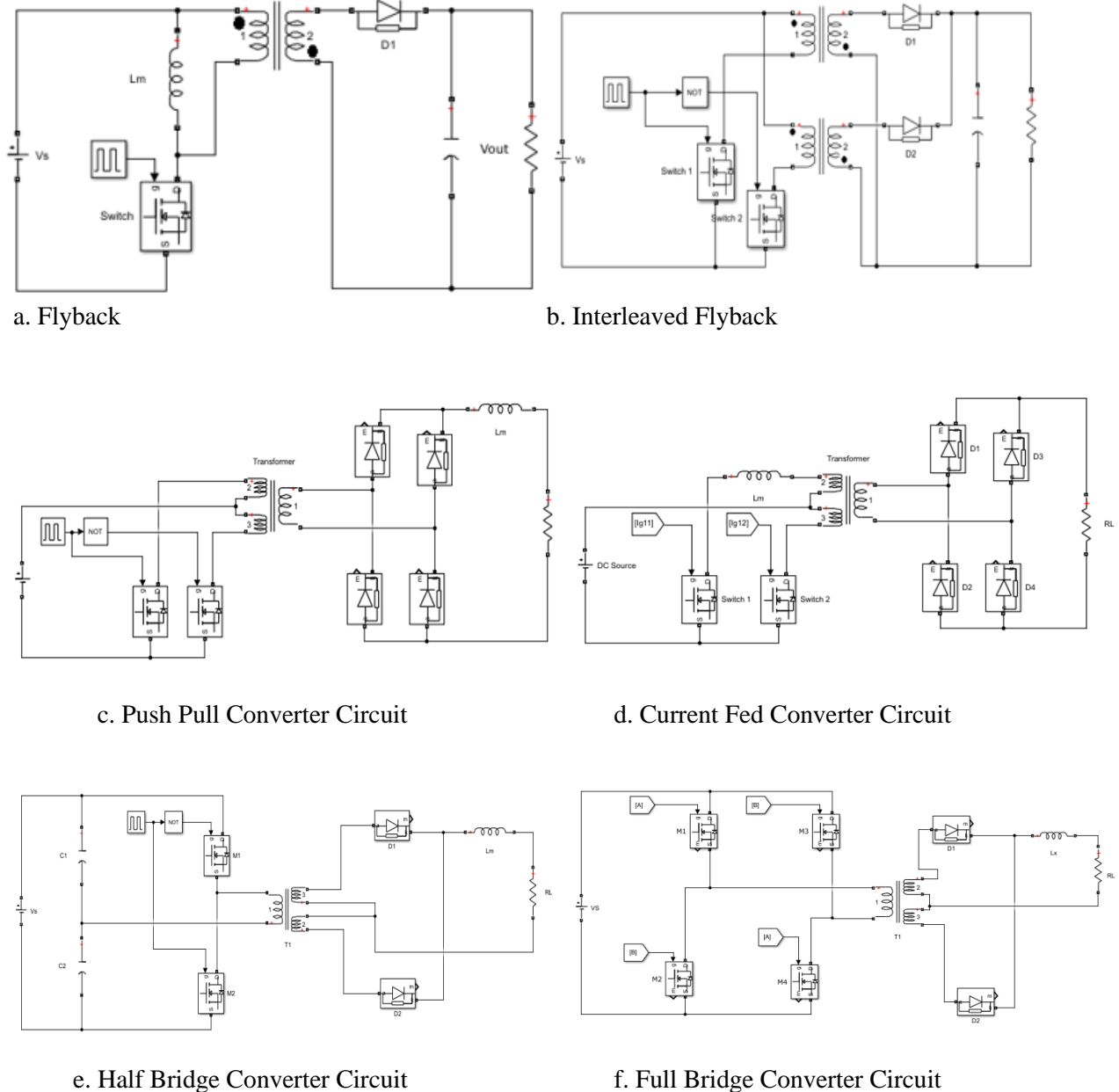


Fig. 2. Six Types of DC-DC Converters

H-BRIDGE INVERTER

Fig. 3. shows the circuit H-Bridge inverter [matlab exchange]. The inverter operates by using MOSFET as switches and the voltage output is produced depending on which switches are closed. The switch connection for this inverter is a combination of S1 and S4 to produce + VDC while S2 and S3 produce -VDC. These switches combination will be on and off alternately. Notice that at the same time, S1 and S2 should not be closed, nor should S3 and S4 be closed as shown in Fig. 4. Otherwise, in the dc sources, a short circuit will occur. True seats are not immediately switched on or off.

Therefore, in the control of the switches, switching transfer times must be accommodated. The overlap of "on" switch times can result in a short circuit across the dc voltage source, often called a shoot-through fault. In this study, Pulse-width modulation (PWM) and

unipolar switching techniques were developed to manage inverter switching. In PWM, with modulating waveforms, the amplitude of the output voltage can be regulated. Two distinct advantages of PWM are reduced filter requirements to minimize harmonics and the regulation of the output voltage amplitude (Adam, 2017). In addition, controlling the switching frequency requires two conditions, namely sinusoidal reference and triangular carrier signal.

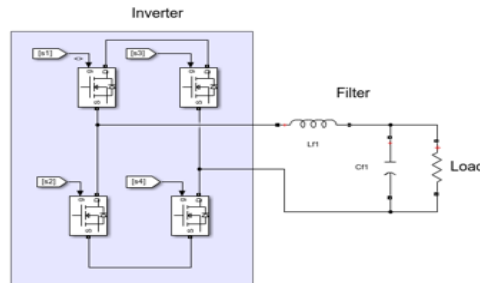


Fig. 3. H Bridge Inverter

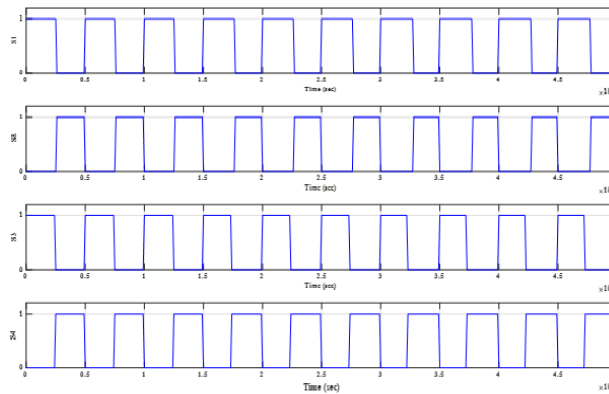


Fig. 4. PWM Signal of Inverter Switching Control

Next, the inverted output signal will be fed into the LC filter to filter out unwanted signals or to reduce harmonics contained in the output inverter voltage. For LC filter design, the value of the inductor is 5mH while the value of the capacitor is 1 μ F.

Table 1. Specification of photovoltaic

No.	Items	Values
1	Maximum Power (W)	175.0914
2	Open Circuit Voltage V_{oc} (V)	43.99
3	Short Circuit Current I_{sc} (A)	5.17
4	The voltage at maximum power point I_{mp} (V)	4.78

MAXIMUM POWERPOINT TRACKER (MPPT)

In this connection, the voltage produced by the PV is 110V. The operation of PV energy conversion systems at the maximum power point (MPP) is crucial for optimizing the output energy of PV arrays. To extract full power from the PV arrays, an MPPT control is necessary.

Perturbation and Observation (P&O) is one of the MPPT techniques used in the designs proposed. This algorithm can be easily implemented using analogue and digital circuitry and requires no prior knowledge of the parameters of the PV generator or measurements of solar intensity and cell temperature. This disrupts the system's operating point, causing the PV array terminal voltage to fluctuate around the MPP voltage, even though the solar irradiance and cell temperature are constant (Hlaili & Mechergui, 2016). In addition,

because of its balance between efficiency and simplicity, it is the most used and the workhorse MPPT algorithm. It suffers, however, from the lack of speed and adaptability needed to track rapid transients under varying environmental conditions (Elgendy et al., 2011).

Fig. 5a. shows a block diagram for reference voltage perturbation in which the PV array output voltage reference is used as the control parameter in conjunction with a PID controller to adjust the duty ratio of the MPPT power converter. When running the scheme at a constant voltage equal to the Standard Test Condition (STC) value of the MPP voltage, the PID controller gains are tuned. These gains are kept constant while the MPPT algorithm regulates the reference voltage.

Fig. 5 b. shows the algorithm block of implementation of P&O by using the method of MPPT with reference voltage control. This algorithm begins with measuring the voltage and current from PV so that its value will be obtained. The MPPT control applied and performed calculations and comparisons with the previous power. Voltage reference obtained by comparison of new voltage, V_{new} and previous voltage, V_{old} .

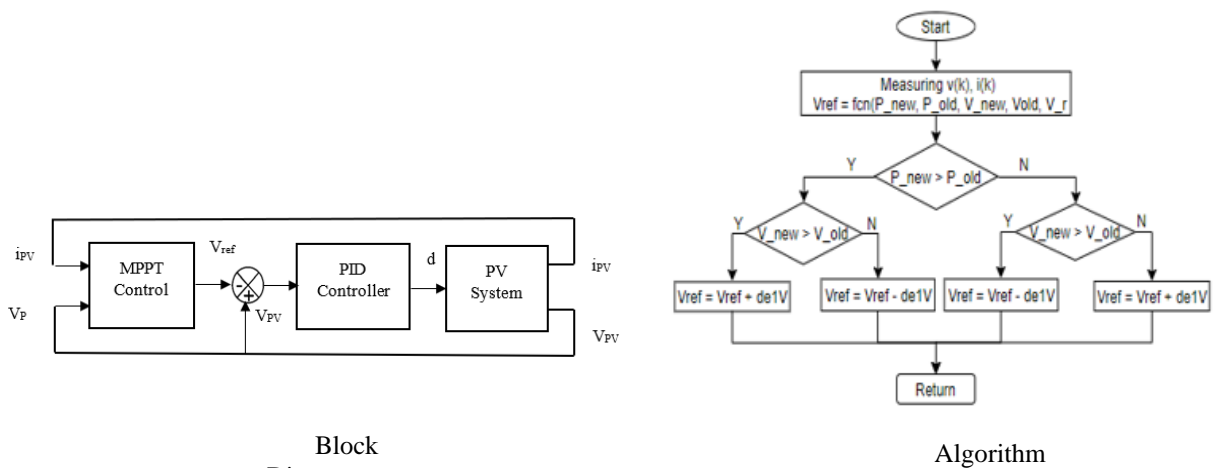


Fig. 5. Implementation of P&O by using the method of MPPT with reference voltage control

For direct duty ratio perturbation, the duty ratio of the MPPT converter is used directly as the control parameter as shown in Fig. 6a. (Malek & Chen, (2014). Direct duty cycle control is the simplest and most effective way to implement the MPPT algorithm. It controls the duty cycle from the error produced by reference and the actual value sensed by the controller. Fig. 6b. shows the algorithm block of P&O by using MPPT with the direct duty ratio control method. Photovoltaic voltage and current are sensed to implement the MPPT algorithm. The MPPT control applied and performed calculations and compared the change of power to the zero value. The reference measure determines the duty cycle of the switching MOSFET to control the charging current. Based on the error sign, the duty cycle either increases or decreases.

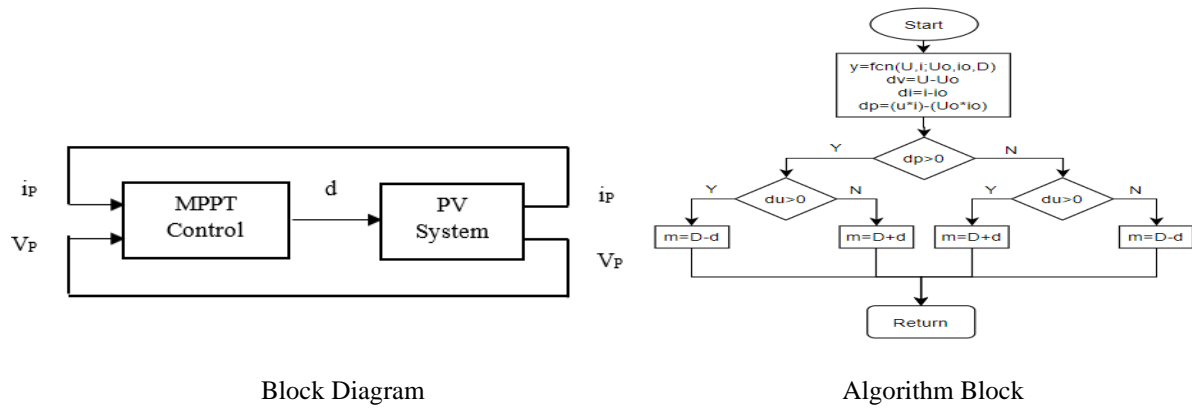


Fig. 6. Implementation of P&O by using the method of MPPT with direct duty ratio control

In this study, the reference voltage control method is applied to control the Interleaved flyback dc-dc converter, Push-pull dc-dc converter, Current-fed dc-dc converter Half-bridge dc-dc converter, and Full-bridge dc-dc converter while the direct duty ratio control method is applied for Flyback dc-dc converter.

RESULTS

IEEE 1547 guidelines set a maximum of 1% or less of the valued current output and percentage of THD to be sustained at a low level in which THD is not to reach 5% (Photovoltaics & Storage, 2009). The lowest percentage of THD in power systems is good because it means efficiency is highest. THD can increase the current in power systems which causes high temperatures in distribution transformers (Elgendy ET AL., 2011). However, keeping low a THD value on a system will further ensure proper operation of equipment and a longer equipment life span.

All these Microinverter designs use MPPT Perturbation and Observation (P&O) type and have been simulated using Simulink MATLAB. Table 2. shows the requirements required to design the six microinverter. The same value used for these 9 items is to get a precise comparison on Microinverters topologies. Obtained the filter values for the selected L_f and C_f are small. The switching frequency of the converter and inverter is high frequency.

Table 2. Requirement of microinverter

No.	Items	Values
1	Filter	$L_f = 5\text{mH}$ $C_f = 1\mu\text{F}$
2	V_{in}	110V
3	V_{DC}	405V
4	V_{out}	230V(rms)
5	I_{out}	0.923A
6	Converter switching frequency	100kHz
7	Inverter switching frequency	20kHz
8	Output frequency	50Hz
9	P_{out}	300W

SIMULATION MICROINVERTERS

Fig. 7. shows the full circuit of the Flyback Microinverter design using MPPT P&O based on Direct Duty Ratio Technique. Fig. 8. shows the full circuit Current-fed Microinverter design using MPPT P&O Reference Voltage Control Technique. The same method is used for Interleaved Flyback, Push-pull, Half-bridge and Full-bridge Microinverters.

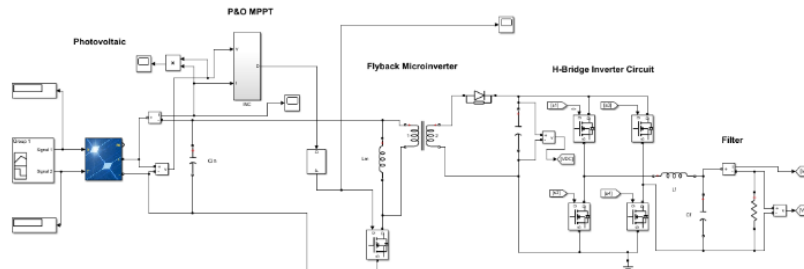


Fig. 7. Flyback Microinverter (Direct Duty Ratio Technique)

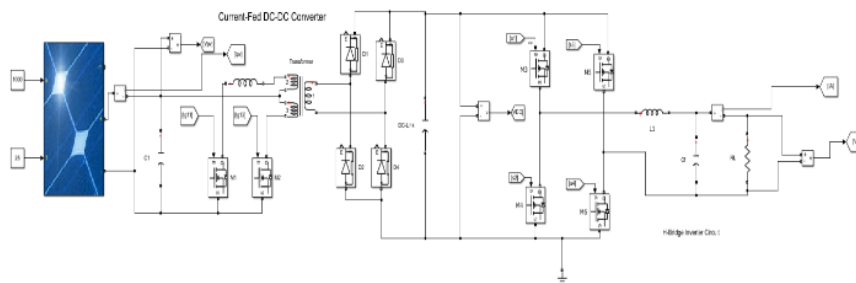


Fig. 8. Current Fed Microinverter (Reference Voltage Control)

Observation to microinverter simulations focuses on waveform which is voltage AC (VAC), the current AC (IAC) and Voltage DC Link (VDC). Then, the important part is to get a low percentage of THD. THD is the summation of all harmonic components of the voltage or current waveform compared to the fundamental component of the voltage or current wave. THD is a measure of the effective value of a distorted waveform of a component harmonize. The result of AC current and voltage is a completely sinusoidal waveform. The observation signal sampling time is between 0.0s to 0.4s with the number of cycles 20 cycles.

Figure 9a. is the output waveform for Flyback. Only in the first cycle, it is found that voltage and current waveform need 0.02s time to stabilize. Figure 10a. shows the spectrum THD of Flyback with 1.24% THD. The spectrum very close appears at 0-15 harmonic order only. Figure 9b. is an output waveform for Interleaved Flyback. The Value of VAC, IAC and VDC are matched with the requirements. The first cycle shows that voltage and current output just need 0.01s time to stabilize. Figure 10b. shows the spectrum THD of Interleaved Flyback with 2.71% THD. The spectrum is scattered in 0-50 harmonic order. Figure 9c. is an output waveform for Push-pull. Observed in the first cycle, the value is less than half value and takes 0.05s time to stabilize. Figure 10c. shows the spectrum THD of Push-pull is 1.47% THD. The spectrum has kept decreasing from 1-20 harmonic order. Figure 9d. is an output waveform for Current-fed. In the first cycle, the value is less than half the same as the output waveform of the Push-pull. In the first cycle, the value is less than half and takes 0.05s time to stabilize. Figure 10d. shows the spectrum THD of the Current fed is 1.26% THD. The spectrum has kept decreasing from 1-20 harmonic order also. Figure 9e. is an output waveform for Half-bridge. In the first cycle, the value is less than half and takes 0.03s time to stabilize. Figure 10e. shows the spectrum THD of Half

Bridge is 2.39% THD. The spectrum is scattered from 0-50 harmonic order. Figure 9f. is an output waveform for the Full bridge. In the first cycle, the value is less than half the same as the output waveform of the Half-bridge. In the first cycle, the value is less than half and takes 0.03s time to stabilize. Figure 10f. shows the spectrum THD of the Full bridge is 2.38% THD. The spectrum is scattered from 0-50 harmonic order.

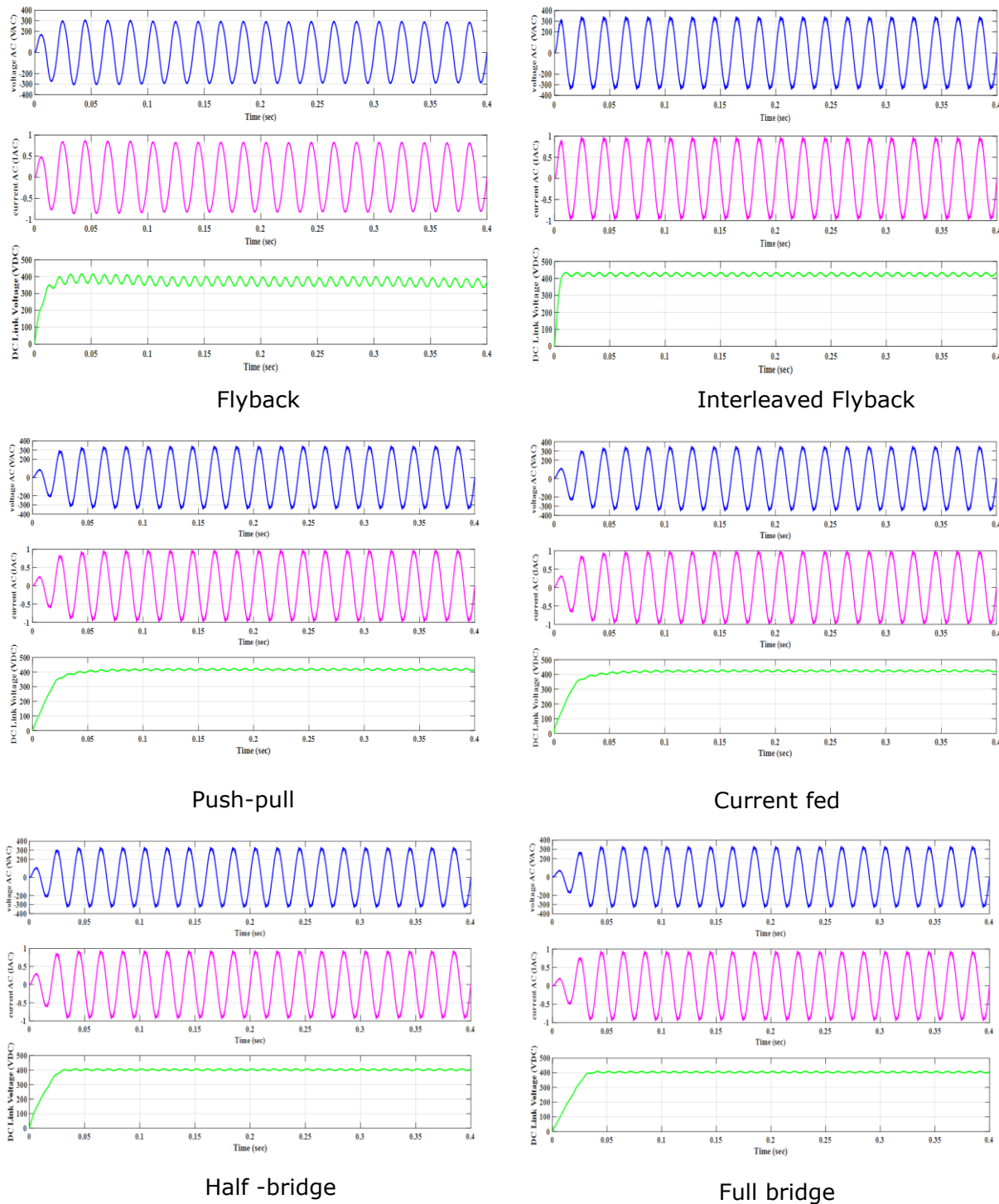
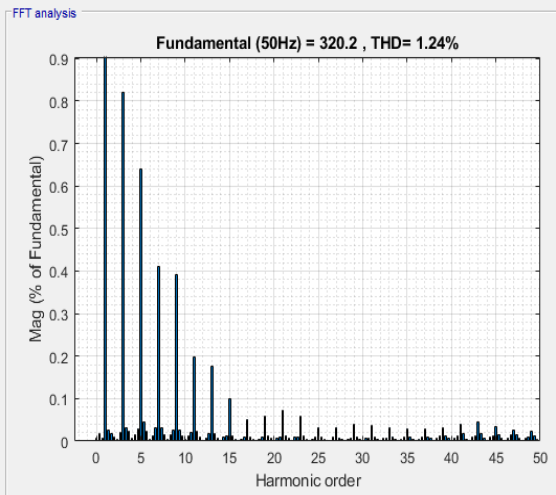
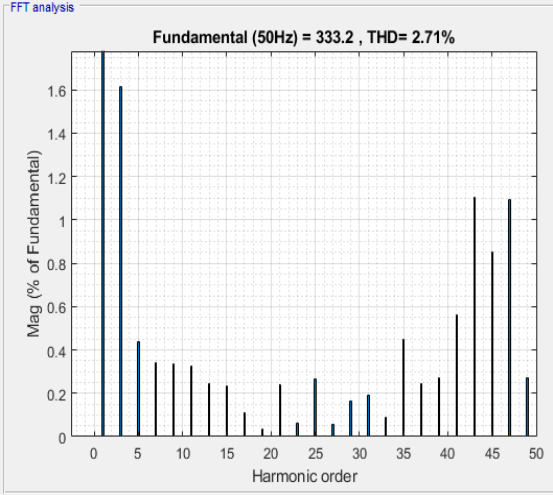


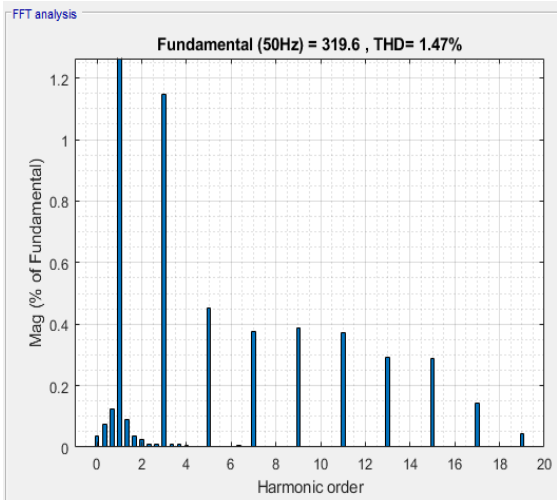
Fig. 9. Waveform of Microinverters



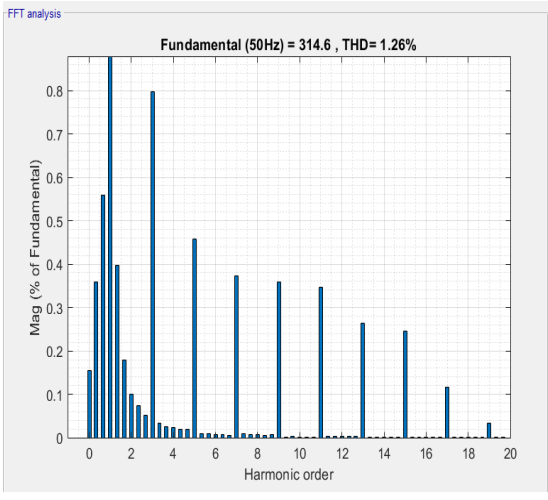
Flyback



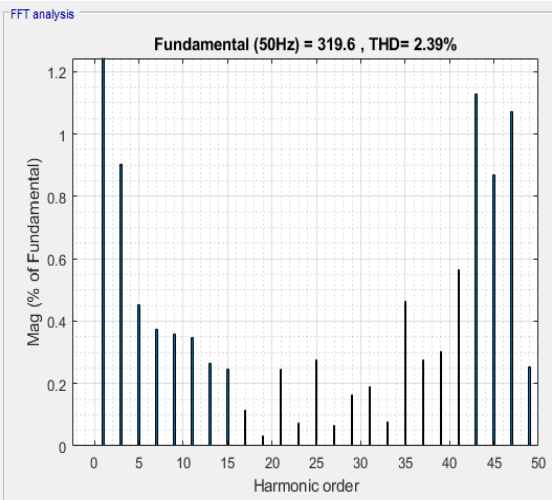
Interleaved Flyback



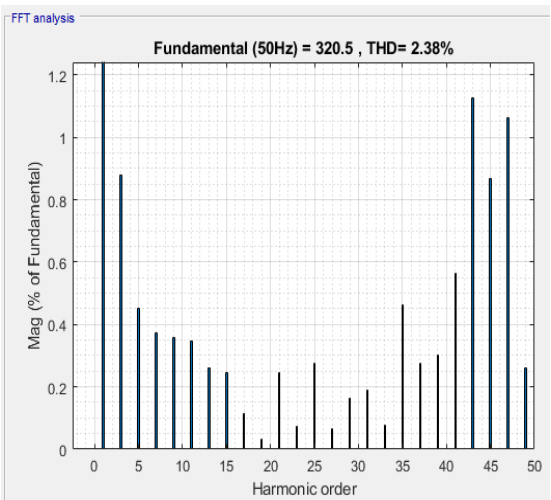
Push Pull



Current Fed



Half Bridge



Full Bridge

Fig. 10. Spectrum THD of Microinverters

Table 3. shows the comparison of six designs of microinverter. The percentage of THD obtained from this simulation is low, which is less than 3%. This shows the lowest percentage of THD is the Flyback microinverter and the highest percentage of THD is Interleaved Flyback microinverter. All microinverters have an output waveform that has a time delay between 0.01s to 0.05s to reach a stable value.

Table 3. Comparison of six design microinverter

The types of microinverter with PV	THD	(N_2/N_1)	Number of components
Flyback microinverter	1.24%	3.7	Mosfet = 1 Capasitor = 2 Inductor = 1 Diode = 1 Transformer = 1
Interleaved flyback microinverter	2.71%	3.3	Mosfet = 2 Capasitor = 2 Inductor = 1 Diode = 2 Transformer = 2
Push-pull microinverter	1.47%	7.7	Mosfet = 2 Capasitor = 2 Inductor = 1 Diode = 4 Transformer = 1
Current-fed microinverter	1.26%	4.3	Mosfet = 2 Capasitor = 2 Inductor = 1 Diode = 4 Transformer = 1
Half-bridge microinverter	2.39%	3.5	Mosfet = 2 Capasitor = 4 Inductor = 1 Diode = 2 Transformer = 1
Full bridge microinverter	2.38%	3.1	Mosfet = 4 Capasitor = 2 Inductor = 1 Diode = 2 Transformer = 1

SUGGESTION

By comparison of six microinverters designed, the Flyback Microinverter was proposed. Due to the value of THD 1.24%, less number of components and the transformer ratio value of 3.7.

CONCLUSION

The microinverter design of this study was the comparison of a multi-stage isolated microinverter that is the combination of a Photovoltaic system, Converter (DC-DC), Inverter (DC-AC), filter, and load. The design type of microinverters produced is Flyback, Interleaved Flyback, Push-Pull, Current-Fed, Half Bridge and Full Bridge. The MPPT used in the design of all microinverters is to control the switching of the converter. This study uses the method of Perturbation and Observation, P&O through two techniques, namely MPPT with reference voltage control and MPPT with direct duty ratio control. All designs made have met the requirements of $V_{out} = 230V$ (rms), $I_{out} = 0.923A$, $P_{out} = 300W$, output frequency = 50Hz and THD value of less than 5%. The designs are using MOSFET as a switch with a frequency value of 100kHz for converter switching and 20kHz for inverter switching. This study proposed the Flyback Microinverter design due to the value of THD, transformer ratio, and the number of components being the best compared to the others.

REFERENCES

- Abd Rahim, N., Elias, M. B. M., Jamaludin, J. B., Rivai, A., Erixno, O., & Zainal F.Y. (2016). Design and Implementation of a Stand-Alone Micro-Inverter with Push-Pull DC/DC Power Converter. *4th IET Clean Energy and Technology Conference (CEAT)*. <https://doi.org/10.1049/cp.2016.1270>
- Aboadla, E. H. E., Khan, S., Habaebi, M. H., Gunawan.B. A., & Tohtayong, M. (2016). Selective Harmonics Elimination technique in single phase unipolar H-Bridge inverter. *Proceeding 14th IEEE Student on Research and Development (SCORED)* (pp. 1-4). IEEE. <https://doi.org/10.1109/SCORED.2016.7810057>
- Amir, A., Amir, A., Che, H. S., Elkhateb, A., & Abd Rahim, N. (2019). Comparative Analysis of High Voltage Gain DC-DC Converter Topologies for Photovoltaic Systems. *Renewable Energy*, 136, 1147-1163. <https://doi.org/10.1016/j.renene.2018.09.089>
- Chen, B., Gu, B., Zhang, L., Zahid, Z. U., Lai, J. S., Liao, Z., & Hao, R. (2014). A high-efficiency MOSFET transformerless inverter for nonisolated microinverter applications. *IEEE Transactions on Power Electronics*, 30(7), 3610-3622. <https://doi.org/10.1109/TPEL.2014.2339320>
- Chen, S. M., Liang, T. J., Yang, L. S., & Chen, J. F. (2010). A cascaded high step-up DC-DC converter with single switch for microsource applications. *IEEE transactions on power electronics*, 26(4), 1146-1153. <https://doi.org/10.1109/TPEL.2010.2090362>
- Dwivedi, S., Jain, S., Gupta, K. K., & Chaturvedi, P. (2018). Modeling and control of power electronics converter system for power quality improvements. Academic Press.
- Elgendy, M. A., Zahawi, B., & Atkinson, D. J. (2011). Assessment of perturb and observe MPPT algorithm implementation techniques for PV pumping applications. *IEEE transactions on sustainable energy*, 3(1), 21-33. <https://doi.org/10.1109/TSTE.2011.2168245>
- Hasan, R., & Mekhilef, S. (2017). Highly efficient flyback microinverter for grid-connected rooftop PV system. *Solar Energy*, 146, 511-522. <https://doi.org/10.1016/j.solener.2017.03.015>
- Hasan, R., Mekhilef, S., Seyedmahmoudian, M., & Horan, B. (2017). Grid-connected isolated PV microinverters: A review. *Renewable and Sustainable Energy Reviews*, 67, 1065-1080. <https://doi.org/10.1016/j.rser.2016.09.082>

- Huber, L., & Jovanovic, M. H. (1999). Forward-flyback converter with current-doubler rectifier: analysis, design, and evaluation results. *IEEE Transactions on Power Electronics*, 14(1), 184-192. Luz Yolanda Toro Suarez Total Harmonic Distortion and Effect in Electrical Power System *Associate Power Technologies 2015*. <https://doi.org/10.1109/63.737607>
- Hlaili, M., & Mechergui, H. (2016). Comparison of different MPPT algorithms with a proposed one using a power estimator for grid connected PV systems. *International Journal of Photoenergy*, 2016. <https://doi.org/10.1155/2016/1728398>
- Latran M, B., & Teke A. (2015). Investigation of multilevel multifunctional grid connected inverter topologies and control strategies used in photovoltaic systems. *Renew Sustain Energy Reviews*; 42:361-376. <https://doi.org/10.1016/j.rser.2014.10.030>.
- Malek, H., & Chen, Y. (2014). BICO MPPT: a faster maximum power point tracker and its application for photovoltaic panels. *International Journal of Photoenergy*, 2014.
- Nanou SI, Papathanassiou SA. (2014). Modelling of a PV system with grid code compatibility, *Electric Power System Research* 116:301-10. <https://doi.org/10.1016/j.epsr.2014.06.021>
- Nguyen, B., Zhang, X., Ferencz, A., Takken, T., Senger, R., & Coteus, P (2018, March). Analytic model for power MOSFET turn-off switching loss under the effect of significant current diversion at fast switching events. In 2018 *IEEE Applied Power Electronics Conference and Exposition (APEC)* (pp. 287-291). IEEE. <https://doi.org/10.1109/APEC.2018.8341024>
- Photovoltaics, D. G., & Storage, E. (2009). IEEE Application Guide for IEEE Std 1547™, IEEE Standard for Interconnecting Distributed Resources with Electric Power Systems.
- Pressman, A. I. (1991). *Switching power supply design*. McGraw-Hill. Inc. New York. Selecting DC-Link Capacitance in Power Converter by Adam Childley 10 May 2017 <https://www.Avnet.Com/Wps/Portal/Abacus/Resources/Article/Selecting-Dc-Link-Capacitor-For-Power-Converters/> Retrieve 25 December 2020.
- Tali, M., Obbadi, A., Elfajri, A., & Errami, Y. (2014, October). Passive Filter for Harmonics Mitigation in standalone PV System for non-linear load. In *2014 International Renewable and Sustainable Energy Conference (IRSEC)*, (pp. 499-504). IEEE.
- Wang, D., He, X., & Shi, J. (2009). Design and analysis of an interleaved flyback-forward boost converter with the current auto balance characteristic. *IEEE transactions on power electronics*, 25(2), 489-498. <https://doi.org/10.1109/TPEL.2009.2025762>